Available online at www.sciencedirect.com
SCIENCE DIRECT
ELSEVIER
Polymer 46 (2005) 3838–3846
polymer
www.elsevier.com/locate/polymer

Biaxial orientation in HDPE films: comparison of infrared spectroscopy, X-ray pole figures and birefringence techniques

A. Ajji*, X. Zhang, S. Elkoun

Advanced Materials Design, Industrial Materials Institute, NRC, 75 Boul. de Mortagne, Boucherville, Que., Canada, J4B 6Y4

Received 15 December 2004; received in revised form 22 February 2005; accepted 28 February 2005
Available online 7 April 2005

Abstract

In this study, high-density polyethylene films (HDPE) were produced using different processes (film blowing and biaxial orientation) and processing conditions. The orientation of the films was characterized in terms of their biaxial crystalline, amorphous and global orientation factors using birefringence, Fourier transform infrared spectroscopy (FTIR) using a tilted incidence technique and X-ray pole figures. Evaluation of a simplified FTIR procedure without using the tilted method for the determination of crystalline orientation factors proposed in the literature is also evaluated and assessed. The results indicate that FTIR overestimate the crystalline orientation factors, particularly for the crystalline *a*-axis. Significant discrepancies are also observed for the *b*-axis orientation, which may be due to an overlap of the amorphous contribution and/or saturation of FTIR bands. Those differences are larger for films with low orientation, such as blown films. Amorphous phase orientation from FTIR depends on the band used and is not necessarily in agreement with that determined from combination of X-ray and birefringence.

Keywords: HDPE crystalline and amorphous phases orientation; FTIR spectroscopy; X-ray diffraction pole figures

1. Introduction

The production of oriented films from thermoplastic materials represents a large segment of the polymer industry. In fact, orientation of polymers enhances many of their properties [1–5], particularly mechanical, impact, barrier and optical. Biaxial orientation has the added advantage of allowing this enhancement in both directions. One of the commonly used polymers in biaxial orientation processes is polyethylene (PE). The most widely used biaxial orientation processes for films are the standard film blowing process (such as for PE), tubular film blowing (such as for PP and LLDPE) and cast film biaxial orientation or tentering (PP, PS, PET, etc.).

On the other hand, the structure and orientation developed during these processes have a significant effect on the properties of the films. Different techniques can be used to determine the structure and orientation of the films. Microscopy gives an overall picture of the crystalline morphology (lamellar, spherulitic, etc.), X-ray pole figures yields details of crystalline phase orientation. Fourier transform infrared spectroscopy (FTIR) allows the determination of specific orientation factors for the crystalline and amorphous phases as well as that of trans and gauche conformers and combinations [6], provided that their transition moment angle are known. Finally, birefringence gives the average total orientation. For the particular case of PE, FTIR allows the determination of crystalline axes orientation as well. However, the accuracy and precise significance of the different orientation factors determined from these techniques is to be established, although some studies in the past addressed partially this issue as well as their correlations to structure and properties [7–16].

In fact, it was in the fifties [7–9] that Stein treated the comparison of results from FTIR, X-ray diffraction and birefringence theoretically, with a comparison with a simple hypothetical case [7]. It was until the end of the sixties that Read and Stein [10] made some quantitative comparisons for the case of uniaxial orientation, however, the X-ray

* Corresponding author. Tel.: +1 450 641 5244; fax: +1 450 641 5105.
E-mail address: abdellah.ajji@cnrc-nrc.gc.ca (A. Ajji).

0032-3861/$ - see front matter Crown Copyright © 2005 Published by Elsevier Ltd. All rights reserved.
doi:10.1016/j.polymer.2005.03.002

results were not made in the same laboratory. Even with this fact, already significant discrepancies were observed between the FTIR results for the crystalline *a*-axis and those obtained from X-ray at low orientation levels. Some of the observed discrepancies were attributed to potential differences in films and experimental errors. Desper [11] on the other hand studied PE blown films using also X-ray, birefringence and FTIR spectroscopy. However, in his FTIR measurements, he did not use the tilted technique and hence, had not the contribution coming from the thickness direction to compare properly the orientation factors.

More recently, Kissin [17] developed an approach for the use of FTIR for the determination of biaxial orientation factors for HDPE blown films having a specific structure (row structure) using two FTIR spectra, without the need for tilting the films in order to determine the third spectrum [6]. He compared the results of this approach with WAXD results of a biaxially oriented HDPE films with a row structure and found an acceptable agreement based on White–Spruiell biaxial orientation factors. However, when Herman's orientation factors are used to determine the orientation factors, significant differences can be noted between results from FTIR and X-ray diffraction, which may be due to a compensation between the two independent angles that are involved in the White–Spruiell factors. Krishnaswamy [18] modified slightly Kissin's approach and extended it to LLDPE blown films but did not report systematic comparisons with the FTIR tilted technique nor with WAXD results.

In order to clarify the discrepancies observed above in literature and also following our observations from comparing FTIR and X-ray results on orientation factors in blown films, we carried out an extensive and systematic study on different polyethylenes having different morphologies and histories. Uniaxially oriented, biaxially oriented and blown films of HDPE, LLDPE and LDPE were characterized using X-ray pole figures, FTIR and birefringence. The results obtained for Herman's biaxial orientation factors from the different techniques are compared and discussed. A comparison is also made with the approaches of Kissin and Krishnaswamy mentioned above. This first paper addresses the case of HDPE.

2. Experimental

For blown films, high-density polyethylene (HDPE) film resin, with a melt index of 0.34 and density of 0.955, was used. The films were produced using an extrusion blowing line from Brampton engineering. The extrusion temperature profile ranged from 160 to 200 °C. Different draw down ratios (DDR) and blow up ratios (BUR) were used with thicknesses from 12 to 50 μm. The frost line height was about 70 cm.

Initial samples for biaxial stretching were prepared by cast film extrusion of the same HDPE as above for blown films. The initial thickness was in the range of 0.5–1 mm. The stretching was performed on a Bruckner laboratory biaxial stretcher. The conditions were as follow: stretch rate 10%/s simultaneous, initial sample size 10×10 cm^2 and a stretching temperature of 127 °C. Final draw ratios were: uniaxially stretched to a draw ratio of 4 and biaxially stretched to 4×4.

The morphology of the films was determined using a field emission scanning electron microscope (FE-SEM) with and without etching the films and a minimal coating on the surface.

The global biaxial orientation factors were determined using birefringence. The absolute values of birefringence in the machine-normal and transverse-normal planes were measured by an incident multi-wavelength double beam and photodiode array assembly, combined with an in-house developed software. Details of the technique can be found elsewhere [19,20].

The biaxial orientation factors used in this study are those of Hermans: $f_{j\mathrm{M}}$, $f_{j\mathrm{T}}$ and $f_{j\mathrm{N}}$ in the machine, transverse and normal directions, respectively, for the axis *j*. Relation can be developed between these orientation functions and other measurable quantities such as birefringence. Assuming $\Delta^\circ = n_c - (n_a + n_b)/2$ (about 0.058 for PE) and $\delta^\circ = n_a - n_b$, (about -0.003 for PE) where n_a, n_b and n_c are the refractive indices along the *a*, *b* and *c* axes of the crystalline lattice, the following equations for the crystalline phase can be obtained [6]:

$$(\Delta n_{\mathrm{MN}})_{\mathrm{C}} = 2\Delta^\circ(f_{c\mathrm{M}} - f_{c\mathrm{N}})/3 + \delta^\circ(f_{a\mathrm{M}} - f_{a\mathrm{N}} - f_{b\mathrm{M}} + f_{b\mathrm{N}})/3$$

$$(\Delta n_{\mathrm{TN}})_{\mathrm{C}} = 2\Delta^\circ(f_{c\mathrm{T}} - f_{c\mathrm{N}})/3 + \delta^\circ(f_{a\mathrm{T}} - f_{a\mathrm{N}} - f_{b\mathrm{T}} + f_{b\mathrm{N}})/3$$

The total birefringence is due to the crystalline and amorphous phases in addition to a form birefringence (which is generally negligible), if ϕ is the crystalline content, thus, we can write:

$$\Delta n_{\mathrm{MN}} = \phi(\Delta n_{\mathrm{MN}})_{\mathrm{C}} + (1-\phi)(\Delta n_{\mathrm{MN}})_{\mathrm{A}} + \Delta n_{\mathrm{form}}$$

The indices A and C stand here for amorphous and crystalline phases. It is then possible to determine the crystalline phase birefringence from crystalline axes orientation, and amorphous phase birefringence by subtraction of the crystalline contribution from the total birefringence by using the above-mentioned equations.

In general, the contribution of the *a* and *b* axes orientation to the crystalline birefringence is low compared to that of the *c*-axis because of the intrinsic birefringences and it was assumed negligible for the calculations here. Which will lead to the following simplified equations:

$$(\Delta n_{\mathrm{MN}})_{\mathrm{C}} = 2\Delta^\circ(2f_{c\mathrm{M}} + f_{c\mathrm{T}})/3$$

The crystalline axes orientation factors were determined from wide-angle X-ray diffraction pole figures of (110) and (200) reflections using a Bruker AXS X-rays goniometer equipped with a Hi-STAR two-dimensional area detector.

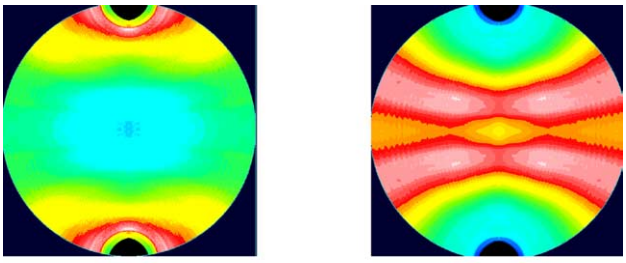

Fig. 1. (200) and (110) crystalline reflections pole figures of HDPE blown films (50 μm films).

The generator was set up at 40 kV and 40 mA and the cu K_α radiation ($\lambda = 1.542$ Å) was selected using a graphite crystal monochromator. Sample to detector distance was fixed at 8 cm. Film samples were stacked to a thickness of about 3 mm in order to obtain enough accuracy in a reasonable time. They were also determined, in addition to those of the amorphous phase, from Fourier transform infrared spectroscopy (FTIR) using the tilted film technique to obtain the spectrum of the normal (film thickness) direction. The measurements were carried out on a Nicolet 170SX FTIR at a resolution of 2 cm^{-1} with an accumulation of 128 scans. Polarization of the beam was performed using a zinc selenide wire grid polarizer from Spectra-Tech. The details on this method were reported elsewhere [6,19].

3. Results

Typical results from X-ray pole figures are shown in Figs. 1 and 2 or blown and biaxially stretched films, respectively. For the blown films, only the (110) and (200) reflections are reported. In fact, evaluation of the crystalline orientation functions using the (020) reflection are not accurate as will be discussed later for biaxially stretched film. For FTIR, typical results in the spectral region of 700–750 cm^{-1} are presented on Fig. 3 for a biaxially oriented film, with the results of the decomposition procedure. Typical films morphologies obtained from SEM are illustrated on Figs. 4 and 5 for both blown and biaxially stretched films. It is clear that a lamellar row nucleated structure has been obtained in all blown films. The quantitative results obtained on the Herman's orientation factors of the crystalline axes as well as the amorphous phase and birefringences are summarized in Tables 1–5 for blown and biaxially stretched films and are discussed in details below.

Lets compare first the crystalline axes orientation determined from FTIR and X-ray pole figures for three blown films of different thicknesses (50, 25 and 12 μm), presented in Table 1. They all agree qualitatively, but in quantitative terms, significant differences are observed. In fact, for the crystalline *a*-axis, the values of the orientation factors in the machine direction (MD) from both techniques confirm that it is oriented towards MD direction for all the films, with much higher values from FTIR, particularly from the 730 and 1471 cm^{-1} vibrations. The 1894 cm^{-1} vibration seems to agree with X-ray results. Read and Stein [10] already reported such differences between the 730 cm^{-1} and X-ray results for low levels of orientation of uniaxially stretched films long time ago. They attributed it to potential overlap with the 720 cm^{-1} band and also to possible uncertainties of X-ray results as a result of thinner films. We do agree with the first argument as is shown in Fig. 3, potential overlap with the amorphous phase band is quite possible, particularly if the peaks are not strong, but also to possible saturation for thick films (absorption higher that 1.7–2 in the FTIR spectrum, note that the spectrum of Fig. 3 is for a biaxially oriented film not a blown film, the latter has a stronger peak for *a*-axis in MD), which may be the case for the MD spectrum of the 50 μm thick film. For the second argument about X-ray results accuracy on thin films, our results were obtained on stacked films with a total thickness of about 3 mm and this error is, we believe, minimal. The argument about peak saturation is in our opinion the most likely for the 50 μm film, and the other argument about potential overlapping of the peaks is valid for all the films. A look on the results on the thinner films shows clearly much smaller differences between FTIR and X-ray results. The 730 and 1471 cm^{-1} bands being of about the same intensities [11], but the 1894 cm^{-1} is weaker also explains the better agreement of the latter with the X-ray results.

For the TD orientation factors of the *a*-axis, the peak due

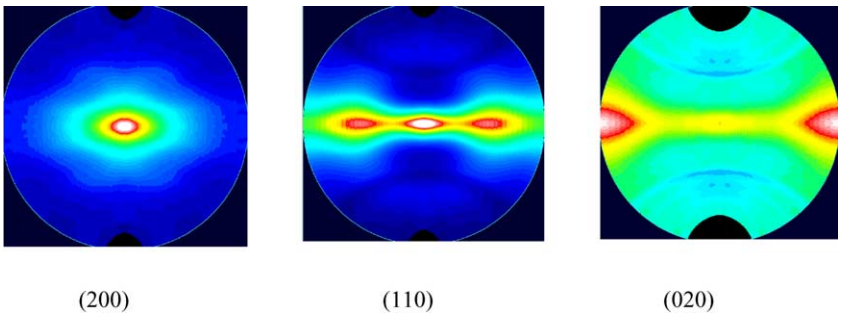

Fig. 2. (200), (110) and (020) crystalline reflections pole figures of HDPE biaxially stretched film to a draw ratio of 4×4.

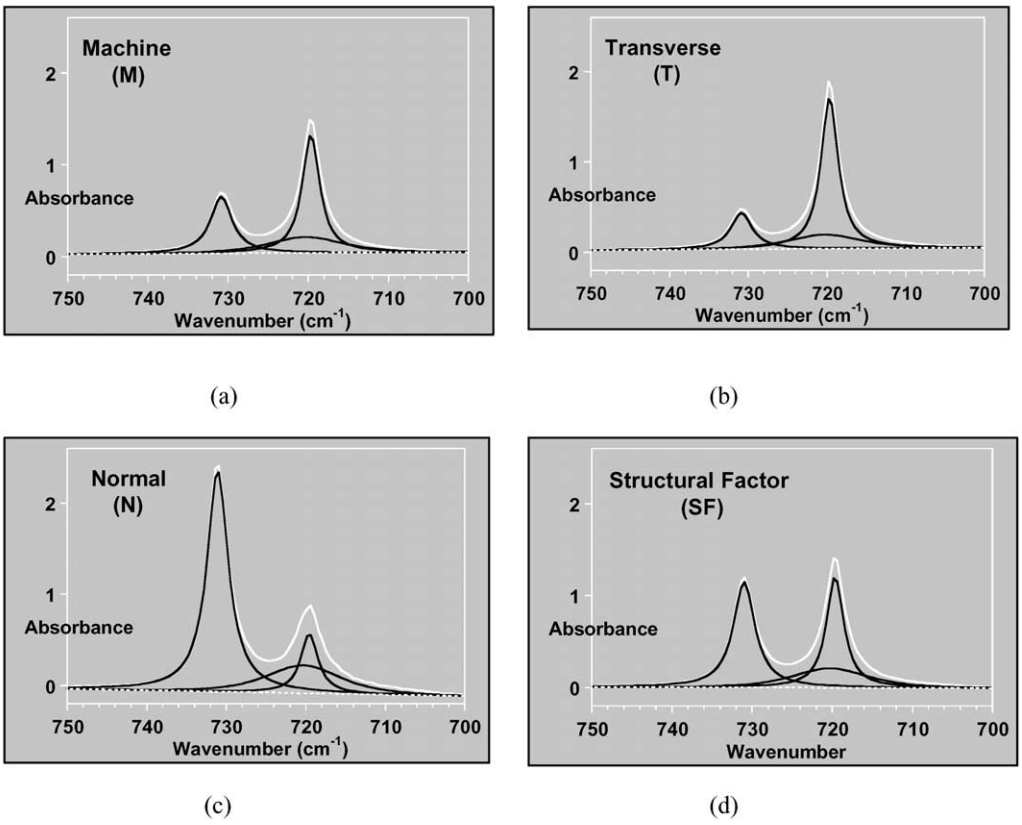

Fig. 3. Typical FTIR spectra and decomposition results in the spectral region of 700–750 cm^{-1} of biaxially stretched HDPE film. (a) Machine direction polarization, (b) transverse direction polarization, (c) normal direction spectrum calculated from the tilted technique method and (d) structural factor spectrum (or unoriented film spectrum).

to the *a*-axis is weaker than in MD, the values are generally low and the differences with those obtained from X-ray are less important, although still FTIR overestimate the orientation. This is most probably due to the overlap of this peak with the amorphous one and partially with the one of the *a*-axis. The results from the 720 and 1464 cm^{-1} bands are quite different in this case for the 50 microns film probably because of a larger overlap.

For the *b*-axis, the values obtained for the orientation factors indicate a preferential orientation in the TD-ND plane for all the films, except for the 50 μm film for which FTIR results suggest an orientation along the TD axis only, in disagreement with X-ray results, as can be seen in Table 1. This latter fact may be due to a possible saturation of *b*-axis band in the TD spectrum. The other discrepancies between the FTIR and X-ray results, particularly for the thinner films, although smaller, may be attributed to the overlap between the amorphous phase and/or *a*-axis peaks.

Now that we know the orientation factors of the crystalline axes for the blown films, some additional analysis is possible in combination with birefringence. The results of measured total birefringence and the one calculated from the crystalline axes orientation factors (using an intrinsic birefringence in the *c*-axis of 0.058) are shown in Table 2 for two blown films. The calculated contribution of the crystalline phase to the total birefringence is also presented (by using the crystallinity results) in Table 2. It is clear from the results that the ones calculated from FTIR orientation factors of the thick film are not acceptable (highly negative birefringences in MD and TD suggest *c*-axis in the normal directions, which is not observed from X-ray results and morphology considerations). This is an additional support of the possible saturation of the peaks in that case. Those obtained for the thinner film or from X-ray results seem reasonable. These results can be used to calculate the amorphous phase orientation and compare the result to the one that can be obtained from various FTIR bands associated with the amorphous phase [10,11]. Those comparisons are presented in Table 3, in addition to global orientation from birefringence and the FTIR 2016 cm^{-1} band [10]. As already stated above, the FTIR results for the crystalline factors of the thick film are not reasonable and their combination with birefringence did again confirm it (orientation factors higher than 1 or lower than −0.5). FTIR bands at 719 cm^{-1} is associated with CH_2 rocking mode of amorphous trans sequences of four or more sequences, 1303 cm^{-1} to CH_2 wagging of GTG conformations which is antisymmetrical with respect to the center of the trans bond, 1352 to CH_2 wagging mode of amorphous

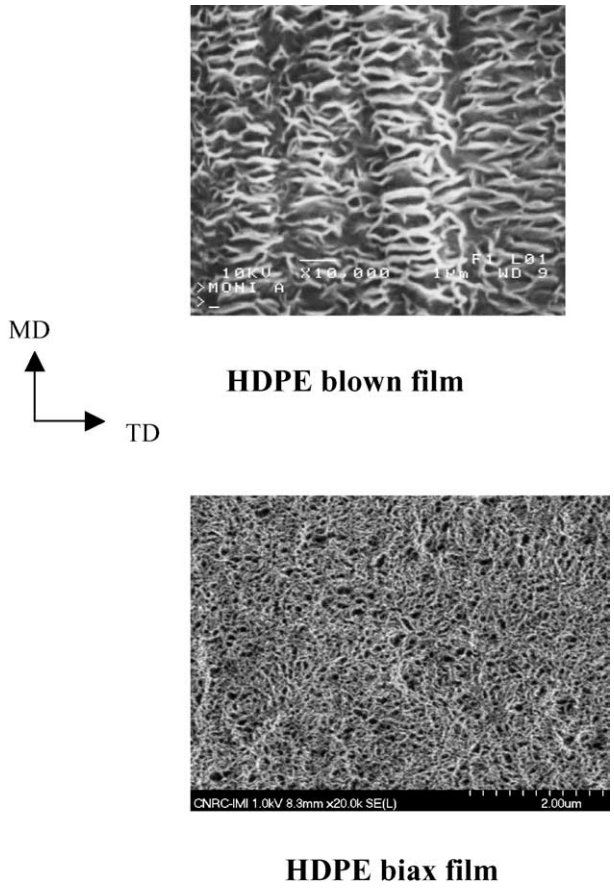

Fig. 4. FE-SEM micrographs of HDPE blown films and a film drawn to 4× 4.

phase segments in the gauche conformations (GG) and 1368 similar to 1303 but symmetrical with respect to the center of the trans bond. The 2016 band is reported for both crystalline and amorphous phases, but with a contribution from extended trans sequences, thus, overestimate the global orientation since it does not contain the gauche contribution, generally lower than the trans one. This can be easily seen in comparing the global orientation from birefringence and the 2016 cm^{-1} band in Table 3. The amorphous orientation factors from the 719 cm^{-1} band are

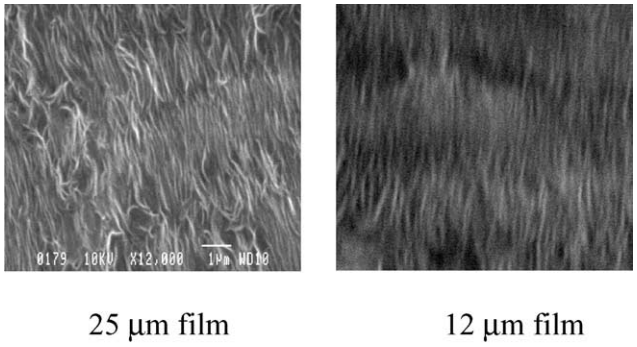

Fig. 5. SEM micrographs of the HDPE blown films used for the evaluation of the simplified FTIR approach.

Table 1
Crystalline orientation factors determined from the different techniques for a blown HDPE film, DDR = 12 and BUR = 2

Film DDR	Technique	MD orientation factors			TD orientation factors			ND orientation factors		
		a-axis	*b*-axis	*c*-axis	*a*-axis	*b*-axis	*c*-axis	*a*-axis	*b*-axis	*c*-axis
DDR 12, BUR 2, 50 μm	FTIR (720–730 cm^{-1})	0.341	−0.208	−0.133	−0.043	0.400	−0.357	−0.298	−0.192	0.490
	(1464–1471 cm^{-1})	0.563	−0.250	−0.313	0.154	0.361	−0.515	−0.716	−0.111	0.827
	a-axis from 1894 cm^{-1}	0.082			0.110			−0.192		
	X-ray	0.096	−0.209	0.113	−0.011	0.095	−0.084	−0.085	0.130	−0.045
DDR 23, BUR 1.6, 25 μm	FTIR (720–730 cm^{-1})	0.257	−0.458	0.201	−0.201	0.283	−0.082	−0.056	0.175	−0.119
	X-ray	0.232	−0.334	0.102	−0.145	0.246	−0.101	−0.087	0.102	−0.015
DDR 4.5, BUR 1.1, 12 μm	FTIR (720–730 cm^{-1})	0.166	−0.470	0.304	−0.141	0.386	−0.245	−0.026	0.084	−0.059
	X-ray	0.066	−0.357	0.292	−0.097	0.309	−0.212	0.031	0.063	−0.094

X-ray results were background and absorption corrected, *b*-axis calculated from (200) and (110) and *c*-axis calculated from *a*-axis and *b*-axis.

Table 2
Measured total birefringence, calculated crystalline birefringence from FTIR and XRD and crystalline contribution to the total birefringence for two selected blown films

Film and crystallinity (%)	Measured total MD birefringence	Measured total TD birefringence	From	Calculated crystalline MD birefringence	Calculated crystalline contribution to total MD birefringence	Calculated crystalline TD birefringence	Calculated crystalline contribution to total TD birefringence
DDR 12, BUR 2, 50 μm	2.3	1.1	FTIR (720–730 cm^{-1})	−24.7	−17.3	−32.4	−22.7
70%			FTIR (1464–1471 cm^{-1})	−44.7	−31.3	−52.3	−36.6
			XRD	5.6	3.9	−1.8	−1.3
DDR 4.5, BUR 1.1, 12 μm	18	8	FTIR (720–730 cm^{-1})	13.3	9.1	−6.8	−4.7
68.7%			XRD	14.5	10.0	−4.2	−2.9

XRD indicate X-ray diffraction.

Table 3
Amorphous and global orientation factors determined from the different techniques for two selected blown films

Film sample and its crystallinity	Global orientation factors from birefringence and FTIR 2016 cm^{-1}, respectively			Amorphous orientation factors from FTIR 722, 1303, 1352, 1368 cm^{-1}, respectively			Amorphous orientation factors from FTIR or X-ray and birefringence		
	f_M	f_T	f_N	f_M	f_T	f_N	f_M	f_T	f_N
DDR 12, BUR 2, 50 μm	0.030	−0.001	−0.029	−0.441	0.178	0.273	0.410	0.830	−1.24[a]
Crystallinity 70%	0.147	0.075	−0.222	−0.264	0.359	−0.095	0.830	1.198	−2.028[b]
				0.096	0.106	−0.202	−0.164	0.193	−0.029[c]
				0.100	0.094	−0.194			
DDR 4.5, BUR 1. 1, 12 μm	0.241	−0.017	−0.224	−0.068	−0.291	0.359	0.103	0.483	−0.586[a]
Crystallinity 68. 7%							0.129	0.411	−0.540[c]

[a] Calculated from FTIR (730–719 cm^{-1} region, Table 1) and birefringence.
[b] Calculated from FTIR (1471–1464 cm^{-1} region, Table 1).
[c] Calculated from X-ray results in Table 1 and birefringence. Only *c*-axis crystalline orientation was taken into account to calculate amorphous orientation.

though to be greatly affected by the decomposition procedure and saturation for the 50 μm film. The 1352 and 1368 bands indicate about the same result for the amorphous, which has been reported also by Read and Stein [10], but different from the one calculated from X-ray and birefringence. The 1303 cm^{-1} band shows the same trend as the calculated values but different in magnitude. Literature results showed, however, that the orientation of this band is the lowest among all the others [10,11]. For the thinner film, the calculated amorphous orientation using FTIR or X-ray results in combination with birefringence are comparable, but different from the ones determined from amorphous 719 cm^{-1} band, which also highlights the difficulties in decomposition of the bands because of overlapping.

For uniaxially and biaxially oriented films, the results obtained for the different crystalline orientation factors are presented on Table 4. Generally, the (020) reflection intensity is weak and for the two films above, the X-ray results were determined using two procedures: (1) *a*-axis from (200), *b*-axis from (020) and *c*-axis from the two; or (2) *a*-axis from (200), *b*-axis from the combination of (110) and (200) and *c*-axis from the two. Significant differences can be observed in the table between the two results. A look at the results presented on Table 5 for calculated amorphous phase orientation from the combination of X-ray results and birefringence indicate that most likely, the results from the first procedure (XR1 in the table) are unreasonable (higher than 1 or below −0.5). It is concluded that the results obtained from the second procedure are more accurate and reliable (this was the procedure used for the blown films above). Now if we compare the FTIR results with those of X-ray for the crystalline axes orientation, particularly the 4×4 film sample, some agreement can be seen, the main difference is in the *a*-axis orientation in the TD direction, which is probably due to overlapping and lower intensity for this peak. For the uniaxial film, it was too thick to be analyzed using the 720–730 cm^{-1} region and only the *a*-axis orientation from the 1894 cm^{-1} band was obtained and agreed relatively with the X-ray results.

The crystalline *a*-axis orientation is basically in the TD-ND plane for the uniaxially oriented film and in the ND direction for the biaxially oriented one. The *b*-axis is in the TD-ND plane in both cases. For the *c*-axis, both techniques indicate it is located in the MD-TD plane, which is expected.

The results obtained for the measured total birefringence, FTIR measured amorphous orientation, calculated amorphous phase orientation results (from combination of birefringence or 2016 cm^{-1} global orientation with crystalline axes orientation from X-ray or FTIR) and global orientation from birefringence and the 2016 cm^{-1} band are presented on Table 5. For the amorphous phase orientation, basically the same comments and discussion as above for blown films can be said. An interesting result to be mentioned is the agreement on the global orientation from

Table 4
Crystalline orientation factors determined from different techniques for uniaxially and biaxially drawn HDPE films

Sample	Technique	MD orientation factors			TD orientation factors			ND orientation factors		
		a-axis	*b*-axis	*c*-axis	*a*-axis	*b*-axis	*c*-axis	*a*-axis	*b*-axis	*c*-axis
4×	FTIR	−0.500			0.333			0.167		
	X-ray	−0.398	−0.236	0.634	0.194	0.239	−0.433	0.204	−0.003	−0.201
			−0.448	0.846		0.311	−0.505		0.153	−0.357
4×4	FTIR	−0.283	−0.128	0.411	−0.275	0.106	0.169	0.558	−0.057	−0.501
	X-ray	−0.247	−0.113	0.360	−0.034	0.090	−0.056	0.281	0.024	−0.305
			−0.224	0.471		0.147	−0.113		0.093	−0.374

X-ray results were background and absorption corrected, first row of X-ray results indicate *c*-axis calculated from *a*-axis and *b*-axis, second row of X-ray results indicate (020) calculated from (200) and (110). For FTIR spectroscopy results on the uniaxially drawn sample, the *a*-axis orientation was determined from the 1894 cm^{-1} vibration but the *b*-axis orientation could not be determined because of saturation of the different bands associated with it and hence, the *c*-axis orientation could not be determined.

Table 5
Amorphous and global orientation factors determined from the different techniques for the uniaxially and biaxially drawn HDPE films

					Film sample	Crystallinity (%)	f_M	f_T	f_N	
Amorphous orientation factors from FTIR bands of: 1303 cm^{-1}, amorphous trans 1368 cm^{-1}, amorphous trans					4×	79.2	0.131 0.060	0.001 −0.060	−0.132 0.000	
Amorphous orientation factors from FTIR band of: 720 cm^{-1}					4×4	80.6	0.166	−0.420	0.254	
Calculated amorphous orientation		f_M			f_T			f_N		
		XR1	XR2	FTS	XR1	XR2	FTS	XR1	XR2	FTS
Calculated amorphous orientation from X-ray or FTIR and global orientation (from birefringence or FTIR band at 2016 cm^{-1})	4× (brief)	0.942	0.135	–	0.033	0.308	–	−0.975	−0.443	–
	4× (2016)	1.023	0.216	–	−0.414	−0.140	–	0.609	−0.076	–
	4×4 (brief)	0.747	0.285	0.535	−0.257	−0.020	−1.192	−0.485	−0.199	0.329
Average orientation				Crystallinity (%)		Δn_{MN} and/or f_M		Δn_{TN} and/or f_T		Δn_{MT} and/or f_N
Measured total birefringence and global orientation from measured birefringence and from 2016 cm^{-1}	4× (brief)			79.2		41.0, 0.698		1.0, −0.336		40, −0.362
	4×2016 cm^{-1}			79.2		0.715		−0.429		−0.286
	4×4 (brief)			80.6		30.0, 0.435		9.5, −0.095		20.5, −0.340

$\Delta^\circ = 0.058$ for HDPE crystalline and amorphous phases. Just *c*-axis contribution was considered in global orientation.

Table 6
Comparison of the simplified FTIR approach with the full calculations approach and X-ray diffraction results

Technique	$f_{a,MD}$	$f_{b,MD}$	$f_{c,MD}$	$f_{a,TD}$	$f_{b,TD}$	$f_{c,TD}$	$f_{a,ND}$	$f_{b,ND}$	$f_{c,ND}$
25 μm HDPE film									
XRD	0.232	−0.334	0.102	−0.145	0.246	−0.101	−0.087	0.102	−0.015
FTIR tilted technique full calculations	0.257	−0.458	0.201	−0.201	0.283	−0.082	−0.056	0.175	−0.119
FTIR simplified approach	0.257	−0.436	0.180	−0.201	0.270	−0.068	−0.056	0.166	−0.110
12 μm HDPE film									
XRD	0.066	−0.357	0.292	−0.097	0.309	−0.212	0.031	0.063	−0.094
FTIR tilted technique full calculations	0.166	−0.470	0.304	−0.141	0.386	−0.245	−0.026	0.084	−0.059
FTIR simplified approach	0.166	−0.459	0.293	−0.141	0.377	−0.236	−0.025	0.082	−0.057

birefringence and the 2016 cm^{-1} band for the uniaxially oriented film. This is probably because of the highly oriented nature of the film, which makes the gauche orientation also quite higher and yields higher birefringence, in contrast with films with a low orientation.

As mentioned in the introduction, a simplified FTIR procedure without the use of the tilted technique has been proposed in literature for [17,18] for film possessing the row structure. Details of the procedure can be found in Refs. 17,18. Our purpose here is to compare this procedure with the full FTIR procedure that uses the tilted technique and compare both results with X-ray diffraction. First, the morphology has to be of the row-nucleated type, which is the case as illustrated for the blown films in Figs. 4 and 5. We consider here only the thin blown films of 12 and 25 μm in order to avoid any peak saturation. The results are presented in Table 6 for the crystalline axes orientation factors. It is clearly seen that the two FTIR procedures give similar results, but both are different from those obtained from X-ray diffraction as discussed above. This is a confirmation of the validity of the simplified procedure in the limits of its validity, but one should be aware that the results are different from those from X-ray diffraction and, if you do not have a row nucleated morphology, the results of the two FTIR procedures are completely different as will be shown in a forth coming paper on linear low density polyethylene (LLDPE).

Finally, in determining the biaxial orientation factors of polyethylenes using different techniques, one should be careful in their interpretation. FTIR may overestimate significantly *a*-axis orientation, decomposition of the different contributions may be difficult and peaks may saturate even for quite thin films. Amorphous phase orientation determination may be significantly affected by peaks overlap.

References

[1] Yu TH, Wilkes GL. Polymer 1996;37:4675.
[2] McRae MA, Maddams WF. J Appl Polym Sci 1978;22:2761.
[3] Choi KJ, Spruiell JE, White JL. J Polym Sci: Polym Phys Ed 1982;20:27.
[4] Kanetsuna H. J Appl Polym Sci 1978;22:2707.
[5] Matthews RG, Duckett RA, Ward IM, Jones DP. Polymer 1997;38:4795.
[6] Cole KC, Ajji A. Characterization of orientation. In: Ward IM, Coates PD, Dumoulin MM, editors. Solid phase processing of polymers. Munich: Carl Hanser Verlag; 2000.
[7] Stein RS, Norris FH. J Polym Sci 1956;21:381.
[8] Stein RS. J Polym Sci 1958;31:327.
[9] Stein RS. J Polym Sci 1958;31:335.
[10] Read BE, Stein RS. Macromolecules 1968;116.
[11] Desper CR. J Appl Polym Sci 1969;13:169.
[12] Zhang XM, Verilhac JM, Ajji A. Polymer 2001;42:8179.
[13] Lindenmeyer PH, Lustig S. J Appl Polym Sci 1965;9:227.
[14] Desper CR, Stein RS. J Appl Phys 1966;37:3990.
[15] Read BE, Hughes DA. Polymer 1972;13:495.
[16] Maddams WF, Preedy JE. J Appl Polym Sci 1978;22:2721–59.
[17] Kissin YV. J Polym Sci, Part B: Polym Phys 1992;30:1165.
[18] Krishnaswamy RK. J Polym Sci, Part B: Polym Phys 2000;38:182.
[19] Ajji A, Guevremont J, Matthews RG, Dumoulin MM. ANTEC 1998;2:1588.
[20] Ajji A, Guèvremont J. US Patent No. 5, 864, 403; 1999.